RESEARCH ARTICLE

Degradation of benzo[*a*]pyrene by bacterial isolates from human skin

Juliane Sowada[1], Achim Schmalenberger[2], Ingo Ebner[1], Andreas Luch[1] & Tewes Tralau[1]

[1]Department for Product Safety, German Federal Institute of Risk Assessment (BfR), Berlin, Germany; and [2]Department of Life Sciences, University of Limerick, Limerick, Ireland

Correspondence: Tewes Tralau, German Federal Institute of Risk Assessment (BfR), Department for Product Safety, Max-Dohrn-Strasse 8-10, 10589 Berlin, Germany.
Tel.: +49 (0) 30-18412-3842;
fax: +49 (0) 30-18412-4928;
e-mail: tewes.tralau@bfr.bund.de

Received 24 September 2013; revised 12 December 2013; accepted 20 December 2013. Final version published online 21 January 2014.

DOI: 10.1111/1574-6941.12276

Editor: Tillmann Lueders

Keywords
benzo[a]pyrene; bacterial degradation; carbon limit; human skin; microbiome; polycyclic aromatic hydrocarbons.

Abstract

Polycyclic aromatic hydrocarbons (PAHs) are some of the most widespread xenobiotic pollutants, with the potentially carcinogenic high-molecular-weight representatives being of particular interest. However, while in eukaryotes, the cytochrome P450 (CYP)-mediated activation of benzo[*a*]pyrene (B[*a*]P) has become a model for metabolism-mediated carcinogenesis, the oxidative degradation of B[*a*]P by microorganisms is less well studied. This should be reason for concern as the human organ most exposed to environmental PAHs is the skin, which at the same time is habitat to a most diverse population of microbial commensals. Yet, nothing is known about the skin's microbiome potential to metabolise B[*a*]P. This study now reports on the isolation of 21 B[*a*]P-degrading microorganisms from human skin, 10 of which were characterised further. All isolates were able to degrade B[*a*]P as sole source of carbon and energy, and degradation was found to be complete in at least four isolates. Substrate metabolism involved two transcripts that encode a putative DszA/NtaA-like monooxygenase and a NifH-like reductase, respectively. Analysis of the 16S-rRNA genes showed that the B[*a*]P-degrading isolates comprise Gram$^+$ as well as Gram$^-$ skin commensals, with *Micrococci* being predominant. Moreover, microbial B[*a*]P-degradation was detected on all volunteers probed, indicating it to be a universal feature of the skin's microbiome.

Introduction

Polycyclic aromatic hydrocarbons (PAHs) are amongst the most ubiquitous xenobiotics found in the environment. As pollutants the majority is of anthropogenic origin such as petrochemicals or as byproducts of combustion (Mohn *et al.*, 1997; Morillo *et al.*, 2007). Following metabolic activation many of them are proven or suspected carcinogens and have hence been in the focus of toxicological and environmental research alike (Cerniglia, 1993; Baird *et al.*, 2005; Johnsen *et al.*, 2005; Shimada, 2006; Husain, 2008; Peng *et al.*, 2008; Haritash & Kaushik, 2009; Luch & Baird, 2010; Harms *et al.*, 2011). Especially the multicyclic high-molecular-weight PAHs suffer from poor biodegradability and have at the same time a tendency to form carcinogenic intermediates (Kanaly & Harayama, 2000; Moody *et al.*, 2004; Haritash & Kaushik, 2009). Much of our current knowledge has been gathered using two model substances, naphthalene and benzo[*a*]pyrene (B[*a*]P). The first was the substrate of choice for numerous microbial biodegradability studies (Heitkamp *et al.*, 1987; Juhasz & Naidu, 2000; Kimura *et al.*, 2006; Toledo *et al.*, 2006; Peng *et al.*, 2008; Jones *et al.*, 2011b), while the latter has been of particular interest as a typical cytochrome P450 (CYP)-activated carcinogen in eukaryotes (Supporting Information, Fig. S1a) (Dekant, 2009). The predominant phase I metabolite of B[*a*]P is the electrophilically reactive and thus unstable B[*a*]P-7,8-epoxide. Its subsequent enzymatic hydrolysis by microsomal epoxide hydrolase (mEH) typically leads to the formation of the B[*a*]P-7,8-dihydrodiol, which is then further oxidised to the B[*a*]P-7,8-dihydrodiol-9,10-epoxide (Baird *et al.*, 2005). As an electrophile, the latter can either be substrate for glutathione-*S*-transferases or is

prone to react with DNA bases such as guanine, forming DNA-adducts. Being a strong carcinogen, B[*a*]P has routinely been assessed from the toxicological perspective but has only rarely been looked at as a potential microbial substrate. The few studies available report on the carbon-limited degradation of B[*a*]P as an environmental pollutant, usually in co-culture or in the presence of cosubstrates such as anthracene, fluoranthene or phenanthrene (Gibson *et al.*, 1975; Mahaffey *et al.*, 1988; Juhasz & Naidu, 2000; Moody *et al.*, 2003, 2004; Toledo *et al.*, 2006; Peng *et al.*, 2008; Jones *et al.*, 2011a, b; Vitte *et al.*, 2013). Unlike in eukaryotes, the bacterial metabolism of complex aromatic hydrocarbons routinely involves dioxygenation. For instance, the stepwise oxidative degradation of B[*a*]P in *Mycobacterium vanbaalenii* PYR-1 (Fig. S1b) is befittingly orchestrated by multiple stereospecific mono- and dioxygenases (Kweon *et al.*, 2011). The respective intermediates (i.e. B[*a*]P-4,5-, B[*a*]P-9,10- and B[*a*]P-11,12-dihydrodiol) overlap only partially with those formed in eukaryotes but, unlike the latter, miss any further toxicological characterisation.

This lack of knowledge is worrying as the human organ most exposed to PAHs is the skin, living space of a most diverse population of commensalic microorganisms (Turnbaugh *et al.*, 2007; Costello *et al.*, 2009; Grice *et al.*, 2009). The skin's microbiota comprises more than 1000 bacterial species, which are highly adapted to the various ecological niches of different skin regions (e.g. dry surfaces and sebaceous areas) (Grice *et al.*, 2009; Li *et al.*, 2012). In such a densely populated environment, competition for carbon sources is fierce, and in case of xenobiotics such as B[*a*]P, aerobic growth is likely to promote the formation of potentially toxic metabolites. Therefore, the aim of this study was to assess the potential of the skin's microbiome to degrade B[*a*]P. We now report on the isolation and characterisation of several B[*a*]P-utilising isolates from human skin and show that the respective organisms use different metabolic pathways for substrate degradation. Further on, we identified some of the genes likely to be involved in B[*a*]P-degradation and investigated their prevalence *in situ*.

Materials and methods

Chemicals and media

Chemicals were purchased from Sigma-Aldrich unless stated otherwise. Molecular reagents and kits were routinely obtained from New England BioLabs (NEB, Frankfurt am Main, Germany), MBI Fermentas (Fisher Scientific – Germany GmbH, Schwerte, Germany) or Qiagen (Qiagen, Hilden, Germany). The purity of chemicals used for enrichment cultures was greater than 98%.

Bacterial sample collection, enrichment and identification of pure cultures

Bacterial skin swabs were collected from the volar forearm and the neck of several volunteers. Subjects probed were of different gender and age and were selected to represent various levels of pre-exposure to PAHs. To obtain a representative microbial community, all participants were asked not to wash the respective skin areas for at least 6 h prior to probing. Samples were collected from 4 cm^2 of skin using sterile medical swabs (OmniSwab, Whatman GmbH, Dassel, Germany), which were subsequently used to inoculate carbon-limited enrichment cultures as described previously (Thurnheer *et al.*, 1986; Schläfli Oppenberg *et al.*, 1995; Tralau *et al.*, 2001). Briefly, enrichment was carried out at 30 °C using minimal salts medium with 100 μM B[*a*]P as sole source of carbon and energy. Dimethylsulphoxide (DMSO) was used as solvent at a final concentration of 26 μM. Cultures were set up in parallel using liquid medium and agar plates. Enrichments showing no growth were supplemented with vitamins for a maximum of two passages (Pfennig, 1978). Based on previous experiences, the provision of vitamins can support growth adaptation of slow-growing cultures on minimal salts medium and helps to avoid the isolation of cross-feeding communities (Tralau *et al.*, 2011). Meanwhile, the short-term provision will ultimately warrant the isolation of prototrophic isolates. Rich medium was used for some of the experiments and consisted of lysogeny broth (LB) supplemented with 100 μM B[*a*]P as needed.

Pure cultures of B[*a*]P-degrading isolates were identified according to the sequence of their 16S-rRNA genes as described previously (Tralau *et al.*, 2011). Initial sequence similarities were identified using the NCBI-BLAST search engine (http://blast.ncbi.nlm.nih.gov/) (Altschul *et al.*, 1990). Further phylogenetic analysis was carried out after importing the sequences obtained in this study alongside sequences from the BLAST result and the SILVA 16S-rRNA gene database (Pruesse *et al.*, 2007) into ARB (Ludwig *et al.*, 2004). Phylogenetic trees were calculated after sequence alignment using the maximum-likelihood algorithm RAXML (Stamatakis, 2006) and a 50% base frequency filter.

Bacterial growth

Bacterial growth was routinely estimated using optical density (OD, λ = 600 nm) or based on the increase in soluble protein. The latter was determined according to the method published by Lowry *et al.* (1951).

Cultures for the determination of growth rates and the substrate range were set up as sixfold biological replicates in an incubation plate reader (Synergy HT, Biotek) using

96-well plates. Wells were filled with 200 μL of culture per 300-μL well and incubated with medium shaking at 30 °C. All measurements were subsequently performed as 10-fold technical replicates, and the results were found to be statistically significant within $P \leq 0.05$. Carbon sources were provided either as 100 μM B[*a*]P or as equimolar amount of carbon thereof.

Gas chromatography coupled to mass spectrometry (GC/MS)

GC/MS was used to verify substrate usage. Following culture growth, any B[*a*]P remaining was extracted by liquid–liquid extraction using *n*-hexane as solvent. A total of 1 μL of extract was subsequently injected (splitless, 220 °C) into a GC 8000 gas chromatograph (Fisons Instruments, Manchester, UK) and separated using a DB-5MS UI column (30 m × 0.25 mm × 0.25 μm) (Agilent technologies, Böblingen, Germany). The column was operated with a prepressure of 85 kPa and a temperature gradient ranging from 80 °C (for 1 min) to 300 °C (ramped at 25 °C min^{-1}, for 3 min). Following chromatographic separation B[*a*]P was quantified on an MD 800 mass spectrometer (Fisons Instruments), with the temperature of the transfer capillary being kept at 240 °C.

RT-PCR, PCR, cloning and sequencing

Transcription of genes was probed using reverse transcription-PCR (RT-PCR) and a set of primers that were designed to be specific for conserved genes of bacterial PAH-degradation (Table S1). Pathways targeted comprised the degradation of pyrene, naphthalene, phenanthrene, biphenyl, bisphenol, aromatic alkaloids and various mono- and dioxygenases for the degradation of complex aromatic substances. Primer specificity was tested with PCR using human DNA or genomic DNA of *Escherichia coli* DH5α as negative controls (data not shown). Isolation of mRNA from freshly grown cultures was performed using Qiagen's 'RNeasy Kit' together with Qiashredder for cell lysis and an additional step of on column DNA-digestion (Qiagen). The isolated RNA was quantified spectrophotometrically with a NanoDrop 1000 spectrophotometer (NanoDrop Products, Wilmington), and 1 μg of the isolated RNA was then used for reverse transcription according to Qiagen's 'Omniscript Kit' together with gene-specific primers. The respective cDNA served as template for further PCR-amplification using Taq-polymerase from New England BioLabs (NEB) and the following PCR program: 1 min of predenaturation at 95 °C, followed by 28 cycles of 30 s denaturation at 95 °C, 40 s annealing (refer to Table S1 for the annealing temperature T_a) and 60 s elongation at 72 °C, followed by additional 10 min of postelongation. The reaction buffer contained 1.8 mM $MgCl_2$ and 8.3% (v/v) DMSO.

Amplified DNA fragments were analysed by agarose gel electrophoresis according to Sambrook *et al.* (1989), and the results were documented using a gel documentation system (BioRad Laboratories München, Germany). Fragments specifically transcribed in media containing B[*a*]P were gel-purified ('Qiaquick PCR purification Kit', Qiagen), cloned ('TA-cloning Kit', Invitrogen Life Technologies GmbH, Darmstadt, Germany) and sequenced (MWG-Eurofins, Ebersberg, Germany). All sequences are deposited in GenBank (http://www.ncbi.nlm.nih.gov/genbank/) and are accessible using the following accession numbers: KF993656. KF993657. KF993658. KF993659. KF993660. KF993661. KF993662. KF993663. KF993664. KF993665 (16s-sequences of isolates from the volar forearm), KF993666, KF993667, KF993668, KF993669. KF993670. KF993671, KF993672, KF993673, KF993674, KF993675, KF993676 (16s-sequences of the isolates from the neck).

Nucleic acids isolation from skin swabs

In situ samples of total microbial DNA were isolated directly from skin swabs. Briefly, 4 cm^2 of skin surface was probed using moistened swabs (sample buffer: 100 mM Tris, 2 mM EDTA, pH 7.4), the tips of which were transferred to standard sampling tubes and incubated at in a thermomixer (Eppendorf, Hamburg, Germany) at room temperature for 30 min with 10 000 r.p.m. The resulting cellular suspension was then lysed by passage through a QIAShredder column (Qiagen, Germany) followed by isolation of total genomic DNA with the 'RTP Bacteria DNA Mini Kit' from Invitek (STRATEC Molecular GmbH, Berlin, Germany). The isolated DNA was quantified spectrophotometrically and used as a template for PCR with gene-specific primers (Table S1).

A similar protocol was tried for RNA-isolation but failed to provide sufficient material for downstream application such as RT-PCR. Therefore, RNA was isolated from overnight plates of skin stamps. Samples were taken using patches of filter paper (4 cm^2) soaked in sample buffer and subsequently transferred to LB-agar plates, which were supplemented with 100 μM B[*a*]P. Following overnight incubation at 30 °C, all organisms were then scraped off and subjected to RNA-isolation and RT-PCR as described earlier.

Experiments and results

The potential of the skin's microbiome to metabolise B[*a*]P was tested by setting up carbon-limited enrichment cultures, using skin swabs from several volunteers as inoculum.

Isolation and identification of B[*a*]P-degrading bacteria

Volunteers (n = 11) were selected to represent both genders, various age brackets and different levels of B[*a*]P pre-exposure as projected from lifestyle or occupation. The areas sampled included the volar forearm and the neck, representative of a dry and a sebaceous habitat, respectively. The corresponding enrichment yielded a total of 21 pure cultures, that is, 10 from the volar forearm and 11 from the neck (Table 1). Meanwhile controls inoculated with laboratory surface samples failed to provide B[*a*]P-degrading organisms. Organisms were identified based on BLAST-analysis of the sequence of their 16S-rRNA genes, and their phylogenetic position in a phylogenetic tree (maximum likelihood) was confirmed using ARB (Ludwig *et al.*, 2004) (Fig. 1).

Bacterial degradation of B[*a*]P was found to be a universal feature of the microbiome, with no obvious bias regarding gender, age or pre-exposure. The species isolated most frequently was closely associated with *Micrococcus luteus* (*Actinomycetales*), an obligate saprotrophic aerobe and well-known skin commensal. Its frequency amongst the skin's microbiota has been reported to be lower than 0.5%, with *β-Proteobacteria* and Propionibacteria being the predominant inhabitants of dry and sebaceous areas (Gao *et al.*, 2007; Grice *et al.*, 2009). Other organisms were closely associated with *Staphylococcus caprae*, *Staphylococcus* sp., *Bacillus licheniformis*, *Paracoccus yeei*, *Pseudomonas oleovorans* and *Acinetobacter lwoffii* for the volar forearm and *B. pumilus*, *S. aureus* and *Pantonea agglomerans* for the neck.

Physiological characterisation

The isolates from the volar forearm were subsequently characterised further with hindsight to bacterial growth and substrate range.

Although the use of B[*a*]P as growth substrate was verified for all cultures (Fig. 2), the results show considerable variation with regard to the respective growth rates and mass balances (Table 2). Growth on B[*a*]P tended to be rather slow, with doubling times ranging from 13 h to 3 days. Such slow growth can either be the result of limited transport, slow substrate metabolism or cytotoxicity. However, the latter could be excluded for those cultures where supplementation of LB with B[*a*]P led to increased growth rates (i.e. 3A, 1B, 2B, 3B, 1C, 2C and 1D). With molar growth yields close to 6 g protein per mol carbon, isolates 3A, 3B, 1D and 2D apparently metabolised B[*a*]P completely, while other cultures seemed to be partial degraders. Whereas the analytical identification of any

Table 1. List of B[*a*]P-degrading isolates from the volar forearm and neck

Area sampled	Volunteer	Age [years]	B[*a*]P exposure	Isolate	ID	Sequence identity (%)
Volar forearm	A (♂)	30–40	Medium	1A	*Paracoccus yeei*	99
				2A	*Acinetobacter lwofii*	99
				3A	*Micrococcus luteus*	99
	B (♀)	20–30	Average	1B	*Micrococcus luteus*	99
				2B	*Micrococcus luteus*	99
				3B	*Staphylococcus caprae*	99
	C (♂)	40–50	Average	1C	*Pseudomonas oleovorans*	99
				2C	*Bacillus licheniformis*	99
	D (♂)	0–10	Low	1D	*Micrococcus luteus*	99
				2D	*Staphylococcus* (epidermis)*	99
Neck	E (♀)	20–30	Average	1E	*Micrococcus luteus*	99
	F (♀)	20–30	Average	1F	*Micrococcus luteus*	99
				2F	*Micrococcus luteus*	99
				3F	*Micrococcus luteus*	99
	G (♂)	20–30	High	1G	*Pantoea agglomerans*	100
	H (♂)	20–30	Average	1H	*Bacillus pumilus*	99
	K (♂)	50–60	Medium	1K	*Micrococcus luteus*	99
	L (♂)	30–40	Medium	1L	*Pantoea agglomerans*	99
				2L	*Micrococcus luteus*	99
				3L	*Micrococcus luteus*	99
	M (♂)	0–10	Low	1M	*Staphylococcus aureus*	99

Bacteria were identified according to the sequences of their 16S-rRNA genes. An asterisk designates isolates, which were not clearly identifiable. Pre-exposure to B[*a*]P was projected from the volunteers lifestyle, work environment and self-assessment. 'Average' relates to the exposure expected for a normal office worker, while 'medium' and 'high' designate people who have an increased skin exposure to PAHs on basis of lifestyle or profession (i.e. car mechanics or heavy smoking for medium; tar-handling construction workers for high).

Fig. 1. Phylogeny of B[*a*]P degrading organisms isolated from the volar forearm and the neck. Trees of the 16S rRNA gene were calculated using maximum likelihood (RAXML) and a 50% base frequency filter in ARB based on the ribosomal small subunit database from 2004 and selected sequences imported directly from initial BLAST results and the SILVA RNA database project. Further, information associated with sequences such as strain ID or repository information is provided within square brackets.

metabolites remaining or excreted is pending, preliminary screens indicate some of the supernatants to be potentially cytotoxic (data not shown).

The subsequent characterisation of the substrate range showed that several isolates were also able to grow on other high-molecular-weight PAHs, including potential intermediates of B[*a*]P-degradation, such as pyrene (4 out of 10) or fluoranthene (4 of 10) (Table 3). However, no growth was observed with naphthalene, phenanthrene or anthracene.

Metabolism of B[*a*]P

Aerobic bacterial degradation of B[*a*]P proceeds via stepwise oxygenation (Kweon *et al.*, 2011). Detailed information about the respective metabolism is scarce though. Hence, transcriptional profiling was applied in order to get access to some of the underlying reactions. Primers used were designed to match conserved sequences from pathways reported or suspected to be involved in the degradation of various high-molecular-weight PAHs (Table S1). The screen identified two transcripts that were specifically induced during growth on B[*a*]P (Table 4). Subsequent sequencing confirmed the corresponding mRNAs to encode an uncharacterised flavin-dependent monooxygenase with sequence similarities to DszA/NtaA-like monooxygenases (e.g. 99% to YP_002956349.1 in *M. luteus* NCTC2665 or 80% to YP_702845.1 in *Rodococcus jostii* RHA1) and a NifH-like reductase (100% similarity in several uncultured bacteria).

The transcriptional pattern suggested the respective genes to be involved in B[*a*]P-metabolism and raised

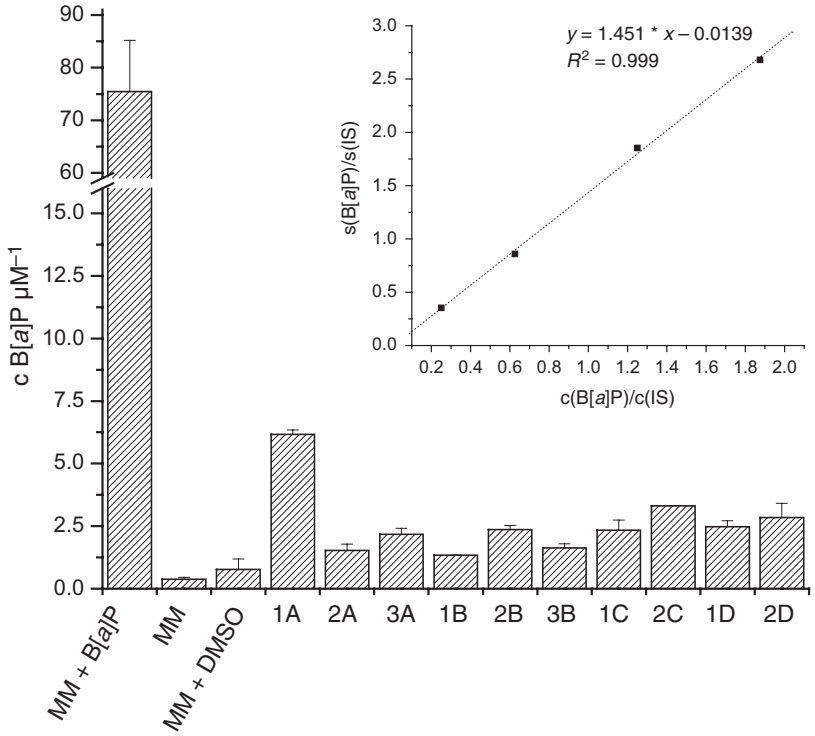

Fig. 2. Use of B[*a*]P by isolates from the volar forearm. Culture supernatants were harvested with onset of the stationary phase and subsequently analysed by GC-MS. The composition of growth media was as follows: MM, minimal medium; MM + B[*a*]P, minimal medium with 100 μM B[*a*]P, MM + DMSO, minimal medium with solvent. All experiments were at least performed in triplicate. Data for the calibration of the GC-MS are shown as inset.

Table 2. Growth parameters of the isolates from the volar forearm

		Doubling time t_D [h]			
Isolate	Organism	LB	LB-B[*a*]P	MM-B[*a*]P	Molar growth yield [g protein per mol C]
1A	*Paracoccus yeei*	8 ± 1	10 ± 1	13 ± 12	0.9 ± 0.1
2A	*Acinetobacter lwofii*	13 ± 4	24 ± 7	18 ± 5	2.6 ± 0.2
3A	*Micrococcus luteus*	5 ± 1	4 ± 0	80	6.5 ± 0.3
1B	*Micrococcus luteus*	5 ± 1	4 ± 0	27 ± 3	2.9 ± 0.6
2B	*Micrococcus luteus*	7 ± 1	6 ± 1	22 ± 5	2.6 ± 0
3B	*Staphylococcus caprae*	8 ± 1	6 ± 1	53 ± 7	4.9 ± 0.4
1C	*Pseudomonas oleovorans*	13 ± 3	7 ± 2	27 ± 1	1.3 ± 0.1
2C	*Bacillus licheniformis*	5 ± 1	5 ± 0	30 ± 4	1.6 ± 0.1
1D	*Micrococcus luteus*	18 ± 2	8 ± 2	37 ± 6	6.4 ± 0.2
2D	*Staphylococcus* (*epidermis*)	5 ± 1	7 ± 1	67*	6.1 ± 0.4

The composition of growth media was as follows: LB, lysogeny broth; LB-B[*a*]P, lysogeny broth with 100 μM B[*a*]P; MM-B[*a*]P, minimal medium with 100 μM B[*a*]P. All experiments were at least performed in triplicate, and the results are statistically significant within $P \leq 0.05$, unless stated otherwise.

*$P > 0.05$.

questions about their abundance and transcriptional activity on human skin. Therefore, PCR was used to probe total microbial DNA isolated from skin swabs (Table 5). The *dszA*/*nta*A-like monooxygenase gene was clearly detectable, while abundance of the gene encoding the NifH-like reductase seemed to be below the detection limit. Transcription *in situ* could not be confirmed due to the limited yields of mRNA obtainable from skin swabs. Nevertheless, some transcripts could be amplified when probing cDNA pools from skin stamps that had been grown overnight on LB supplemented with B[*a*]P (Table 5).

Discussion

This is the first study investigating the degradation of B[*a*]P by the microbiome of the human skin. So far, research on the bacterial degradation of high-molecular-

Table 3. Growth of the isolates from the volar forearm on substrates other than B[*a*]P, lack of growth is designated by a '–'

	Isolates, doubling time t_D [h]									
	1A	2A	3A	1B	2B	3B	1C	2C	1D	2D
Catechol 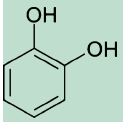	–	15 ± 2	15 ± 2	–	22 ± 1	–	–	–	–	61 ± 10
Salicylic acid 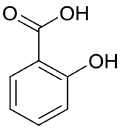	–	–	28 ± 0	58 ± 26*	–	–	–	–	–	–
Phthalic acid 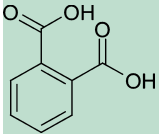	17 ± 1	–	23 ± 6	–	29 ± 16	28 ± 6	–	–	–	21 ± 4
Naphthalene 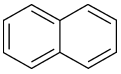	–	–	–	–	–	–	–	–	–	–
Phenanthrene 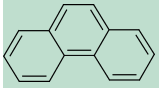	–	–	–	–	–	–	–	–	–	–
Anthracene 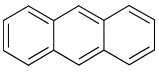	–	–	–	–	–	–	–	–	–	–
Fluoranthene 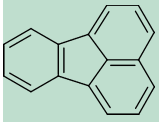	–	–	24 ± 7	20 ± 3	22 ± 8	28 ± 14	–	–	–	–
Pyrene 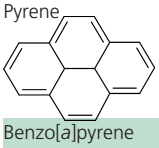	–	24 ± 4	–	59 ± 25*	54 ± 25*	–	24 ± 0	–	–	–
Benzo[a]pyrene 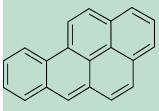	13 ± 12	18 ± 5	73 ± 4	27 ± 3	22 ± 5	53 ± 7	27 ± 1	30 ± 4	37 ± 6	67*

All experiments were at least performed in triplicate, and the results are statistically significant within $P \leq 0.05$, unless stated otherwise.
*$P > 0.05$.

weight PAHs has been focused on their presence as contaminants in the environment, predominantly in soil. Bacterial degradation of B[*a*]P in soils frequently requires mixed communities or the presence of cosubstrates such as phenanthrene, fluoranthene and anthracene. There are only few cultures isolated from soil that grow on B[*a*]P as sole source of carbon and energy (i.e. Gibson *et al.*, 1975; Kweon *et al.*, 2011). The rare occurrence of

Table 4. Transcriptional pattern of fragments generated with primer pairs u50177, u11983 and narAa

		Isolate									
		1A	2A	3A	1B	2B	3B	1C	2C	1D	2D
Primer pair u50177	LB-B[*a*]P	–	–	–	+	–	+	+	+	+	–
– 1159 bp – 1419 bp	MM-B[*a*]P	–	–	+	–	+	–	–	–	–	–
Primer pair u11983	LB-B[*a*]P	+	–	+	+	–	–	–	–	–	–
632 bp 1173 bp	MM-B[*a*]P	–	–	+	–	–	–	–	+	–	–
Primer pair narA	LB-B[*a*]P	–	–	–	–	–	–	+	–	–	–
1406 bp	MM-B[*a*]P	–	–	+	–	–	+	+	–	+	–

Shown are sketches of the sequences used for primer design, the anticipated fragments and the status of detection of the corresponding DNA fragments in the isolates from the volar forearm. The composition of growth media was as follows: LB-B[*a*]P, lysogeny broth with 100 μM B[*a*]P; MM-B[*a*]P, minimal medium with 100 μM B[*a*]P.

Table 5. Presence and transcription of DNA fragments found to be specific for B[*a*]P degradation

		Volunteer			
Fragment	Presence	A	B	C	D
u50177	*In situ*	+	+	+	+
	Ex situ	+	+	+	–
u11983	*In situ*	+	–	+	+
	Ex situ	+	+	+	–
narAa	*In situ*	–	–	–	–
	Ex situ	+	–	+	–

Shown are the PCR results for the total microbial DNA from skin swabs (presence *in situ*) and if transcription of these fragments was detectable on skin stamps after 24 h of incubation on LB supplemented with 100 μM B[*a*]P (transcription *ex situ*, for a representative gel refer to Fig. S2). Samples from sterilised skin areas were used as negative controls.

B[*a*]P-degrading isolates has partly been attributed to fungal enzymes (i.e. CYPs, laccases and peroxidases) being required for the initial activation of B[*a*]P (Harms *et al.*, 2011). Another aspect is that B[*a*]P tends to be only a minor fraction in the complex mixtures of PAHs that constitute the typical xenobiotic load of polluted sites. From a single organism's point of view, this low occurrence is at odds with the energy expenditure and selective pressure required to maintain a complete pathway for B[*a*]P-degradation (Ojo, 2007; Andersson & Hughes, 2010; Haiser & Turnbaugh, 2013).

Still, bacterial B[*a*]P-metabolism seems to be a common feature of the human microbiota as bacteria growing on B[*a*]P could be isolated from the skin of all volunteers. The apparent lack of any bias regarding gender, age or pre-exposure to B[*a*]P points to a high selective pressure for the corresponding pathways and is in line with a permanent exposure of skin to high-molecular-weight PAHs. The most frequent sources of high-molecular-weight PAH-exposure are air-based contaminants (e.g. exhaust fumes or soot) and PAH-contaminations in consumer products (Budavari, 1989; Grob *et al.*, 1991; Dreyer *et al.*, 2005; Morillo *et al.*, 2007; Biedermann & Grob, 2010; Zhao *et al.*, 2011). Examples for the latter include rubber coatings or mineral oils in inks and skin care cosmetics. These can contain up to 0.8% of mineral oil aromatic hydrocarbons (MOAH), comprising substances such as, mostly alkylated, naphthalene, acenaphthylene, acenaphthene, phenanthrene, anthracene, pyrene and fluoranthene derivatives (in house measurements of the German Federal Institute for Risk Assessment, C. Hutzler pers. commun.).

The high abundance of *M. luteus*-like bacteria amongst the isolates is striking (40% and 64% of organisms isolated from the volar forearm and the neck, respectively). According to Grice *et al.* (2009), *Micrococci* comprise less than 4% of the skin's microbiome. At the same time, *M. luteus* is a frequent airborne contaminant and has been isolated from environments as particular as the Herschel Space Observatory (i.e. *M. luteus* strain DSM30505). Yet, the latter could not utilise B[*a*]P as sole source of carbon and energy (data not shown). Similarly, control samples from the laboratory surfaces or aseptically treated skin failed to provide B[*a*]P-degrading organisms. Taken together, these results not only confirm the skin origin of the respective isolates but show *M. luteus* to be a major contributor to PAH-degradation on human skin. Moreover, these findings demonstrate this species' adaptation to a rather challenging nutritional

niche. The respective growth rates were found to vary from 0.03151 h^{-1} to 0.00866 h^{-1}. Such a variation can either be due to varying transport efficiencies or due to the use of different degradation pathways. The latter is supported by differing growth yields for isolates 3A, 1B, 2B and 1D. These indicate complete degradation of B[*a*]P by *M. luteus* 3A and 1D and partial degradation for 1B and 2B. The use of different degradation pathways is supported further by the finding that isolates 3A or 1D utilise just B[*a*]P or B[*a*]P and fluoranthene, while 1B and 2B will also grow on pyrene.

All isolates of the volar forearm were able to use B[*a*]P as sole source of carbon and energy. However, only 40% of them were found to metabolise B[*a*]P completely. For the remaining 60%, the molar growth yields indicate the degradation to be partial. Interestingly, most of the partial degraders accept pyrene as growth substrate. Pyrene is a potential metabolite of B[*a*]P-degradation (Kweon *et al.*, 2011), and its use implies B[*a*]P-degradation to the stage of three aromatic rings or further. It is noteworthy that none of the isolates was able to grow on the possible B[*a*]P-metabolites anthracene, phenanthrene or naphthalene. This could be either due to a lack of metabolism or the absence of suitable transporters.

Transcriptional profiling identified two transcripts that are likely to be involved in B[*a*]P metabolism. According to the BLAST-database, the transcript amplified by the u50177-primer pair encodes a DszA/NtaA-like oxygenase. A search of the sequence database of the 'NIH human microbiome project' (http://www.hmpdacc.org/) confirms this match with skin organisms showing the highest similarities (98% for *M. luteus* SK58 and 79% for *Rhodococcus erythropolis* SK121), followed by commensals from the gut (i.e. *Helicobacter bilis* ATC43879 and *Klebsiella* sp. MS 92-3). The high sequence similarity to *dszA*/*ntaA* points to a monocyclic or ring cleaved substrate, indicating a role during the later stages of B[*a*]P-degradation. In *R. jostii* RHA 1, the corresponding gene is indeed followed by an oxygenase for the breakdown of xenobiotic cyclic terpenes such as limonene. The narAa-primers on the other hand amplified a NifH-like reductase, which was specifically transcribed in the presence of B[*a*]P. As before, it is likely that the respective enzyme catalyses one of the later reactions of B[*a*]P-degradation, similar to the breakdown of the carbon-backbone of chloroalkanes in *Rhodopseudomonas palustris* CGA009 (pathway rpa00625 of the KEGG-database) (Kanehisa *et al.*, 2012). The presence of the respective genes *in situ* was confirmed by their detection in DNA-preparations from bacterial skin swabs, whereas RT-PCR showed their potential transcriptional activity in overnight skin stamps.

Given the frequent exposure of skin to B[*a*]P and other PAHs, it can well be assumed that these substances actually do serve as carbon sources for the skin's microbiota *in situ* and that they are subject to partial as well as complete degradation. In this context the slow growth could prove problematic as it leads to prolonged skin exposure to any intermediates and metabolites excreted. The skin's microbiota has thus to be considered as a potential source for metabolically activated carcinogens.

Acknowledgement

The authors acknowledge intramural funding at the German Federal Institute for Risk Assessment (BfR), Grant 1322-469.

References

Altschul SF, Gish W, Miller W, Myers EW & Lipman DJ (1990) Basic local alignment search tool. *J Mol Biol* **215**: 403–410.

Andersson DI & Hughes D (2010) Antibiotic resistance and its cost: is it possible to reverse resistance? *Nat Rev Microbiol* **8**: 260–271.

Baird WM, Hooven LA & Mahadevan B (2005) Carcinogenic polycyclic aromatic hydrocarbon-DNA adducts and mechanism of action. *Environ Mol Mutagen* **45**: 106–114.

Biedermann M & Grob K (2010) Is recycled newspaper suitable for food contact materials? Technical grade mineral oils from printing inks. *Eur Food Res Technol* **230**: 785–796.

Budavari S (1989) *The Merck Index*. Merck & Co., Rahway, NJ.

Cerniglia CE (1993) Biodegradation of polycyclic aromatic hydrocarbons. *Curr Opin Biotechnol* **4**: 331–338.

Costello EK, Lauber CL, Hamady M, Fierer N, Gordon JI & Knight R (2009) Bacterial community variation in human body habitats across space and time. *Science* **326**: 1694–1697.

Dekant W (2009) The role of biotransformation and bioactivation in toxicity. *EXS* **99**: 57–86.

Dreyer A, Radke M, Turunen J & Blodau C (2005) Long-term change of polycyclic aromatic hydrocarbon deposition to peatlands of eastern Canada. *Environ Sci Technol* **39**: 3918–3924.

Gao Z, Tseng CH, Pei Z & Blaser MJ (2007) Molecular analysis of human forearm superficial skin bacterial biota. *P Natl Acad Sci USA* **104**: 2927–2932.

Gibson DT, Mahadevan V, Jerina DM, Yogi H & Yeh HJ (1975) Oxidation of the carcinogens benzo[*a*]pyrene and benzo[*a*]anthracene to dihydrodiols by a bacterium. *Science* **189**: 295–297.

Grice EA, Kong HH, Conlan S *et al.* (2009) Topographical and temporal diversity of the human skin microbiome. *Science* **324**: 1190–1192.

Grob K, Biedermann M, Caramaschi A & Pacciarelli B (1991) LC-GC analysis of the aromatics in a mineral oil fraction: batching oil for jute bags. *J High Resolut Chromatogr* **14**: 33–39.

Haiser HJ & Turnbaugh PJ (2013) Developing a metagenomic view of xenobiotic metabolism. *Pharmacol Res* **69**: 21–31.

Haritash AK & Kaushik CP (2009) Biodegradation aspects of polycyclic aromatic hydrocarbons (PAHs): a review. *J Hazard Mater* **169**: 1–15.

Harms H, Schlosser D & Wick LY (2011) Untapped potential: exploiting fungi in bioremediation of hazardous chemicals. *Nat Rev Microbiol* **9**: 177–192.

Heitkamp MA, Freeman JP & Cerniglia CE (1987) Naphthalene biodegradation in environmental microcosms: estimates of degradation rates and characterization of metabolites. *Appl Environ Microbiol* **53**: 129–136.

Husain S (2008) Literature overview: microbial metabolism of high molecular weight polycyclic aromatic hydrocarbons. *Remediation* **18**: 131–161.

Johnsen AR, Wick LY & Harms H (2005) Principles of microbial PAH-degradation in soil. *Environ Pollut* **133**: 71–84.

Jones MD, Singleton DR, Sun W & Aitken MD (2011a) Multiple DNA extractions coupled with stable-isotope probing of anthracene-degrading bacteria in contaminated soil. *Appl Environ Microbiol* **77**: 2984–2991.

Jones MD, Crandell DW, Singleton DR & Aitken MD (2011b) Stable-isotope probing of the polycyclic aromatic hydrocarbon-degrading bacterial guild in a contaminated soil. *Environ Microbiol* **13**: 2623–2632.

Juhasz AL & Naidu R (2000) Bioremediation of high molecular weight polycyclic aromatic hydrocarbons: a review of the microbial degradation of benzo[a]pyrene. *Int Biodeterior Biodegradation* **45**: 57–88.

Kanaly RA & Harayama S (2000) Biodegradation of high-molecular-weight polycyclic aromatic hydrocarbons by bacteria. *J Bacteriol* **182**: 2059–2067.

Kanehisa M, Goto S, Sato Y, Furumichi M & Tanabe M (2012) KEGG for integration and interpretation of large-scale molecular data sets. *Nucleic Acids Res* **40**: D109–D114.

Kimura N, Kitagawa W, Mori T, Nakashima N, Tamura T & Kamagata Y (2006) Genetic and biochemical characterization of the dioxygenase involved in lateral dioxygenation of dibenzofuran from *Rhodococcus opacus* strain SAO101. *Appl Microbiol Biotechnol* **73**: 474–484.

Kweon O, Kim SJ, Holland RD *et al.* (2011) Polycyclic aromatic hydrocarbon metabolic network in *Mycobacterium vanbaalenii* PYR-1. *J Bacteriol* **193**: 4326–4337.

Li K, Bihan M, Yooseph S & Methe BA (2012) Analyses of the microbial diversity across the human microbiome. *PLoS One* **7**: e32118.

Lowry OH, Rosebrough NJ, Farr AL & Randall RJ (1951) Protein measurement with the Folin phenol reagent. *J Biol Chem* **193**: 265–275.

Luch A & Baird WM (2010) Carcinogenic polycyclic aromatic hydrocarbons. *Comprehensive Toxicology*, Vol. 14 (McQueen CA, Ed),pp. 85–123. Academic Press, Oxford.

Ludwig W, Strunk O, Westram R *et al.* (2004) ARB: a software environment for sequence data. *Nucleic Acids Res* **32**: 1363–1371.

Mahaffey WR, Gibson DT & Cerniglia CE (1988) Bacterial oxidation of chemical carcinogens: formation of polycyclic aromatic acids from benz[*a*]anthracene. *Appl Environ Microbiol* **54**: 2415–2423.

Mohn WW, Westerberg K, Cullen WR & Reimer KJ (1997) Aerobic biodegradation of biphenyl and polychlorinated biphenyls by Arctic soil microorganisms. *Appl Environ Microbiol* **63**: 3378–3384.

Moody JD, Fu PP, Freeman JP & Cerniglia CE (2003) Regio- and stereoselective metabolism of 7,12-dimethylbenz[*a*] anthracene by *Mycobacterium vanbaalenii* PYR-1. *Appl Environ Microbiol* **69**: 3924–3931.

Moody JD, Freeman JP, Fu PP & Cerniglia CE (2004) Degradation of benzo[*a*]pyrene by *Mycobacterium vanbaalenii* PYR-1. *Appl Environ Microbiol* **70**: 340–345.

Morillo E, Romero AS, Maqueda C, Madrid L, Ajmone-Marsan F, Grcman H, Davidson CM, Hursthouse AS & Villaverde J (2007) Soil pollution by PAHs in urban soils: a comparison of three European cities. *J Environ Monit* **9**: 1001–1008.

Ojo OA (2007) Molecular strategies of microbial adaptation to xenobiotics in natural environment. *Biotechnol Mol Biol Rev* **2**: 1–13.

Peng RH, Xiong AS, Xue Y, Fu XY, Gao F, Zhao W, Tian YS & Yao QH (2008) Microbial biodegradation of polyaromatic hydrocarbons. *FEMS Microbiol Rev* **32**: 927–955.

Pfennig N (1978) *Rhodocyclus purpureus* gen. nov. and sp. nov., a ring-shaped, vitamin B_{12}-requiring member of the family *Rhodospirillaceae*. *Int J Syst Bacteriol* **28**: 283–288.

Pruesse E, Quast C, Knittel K, Fuchs BM, Ludwig W, Peplies J & Glockner FO (2007) SILVA: a comprehensive online resource for quality checked and aligned ribosomal RNA sequence data compatible with ARB. *Nucleic Acids Res* **35**: 7188–7196.

Sambrook J, Fritsch EF & Maniatis T (1989) *Molecular Cloning: A Laboratory Manual*. Cold Spring Harbor Laboratory Press, Cold Spring Harbor, NY.

Schläfli Oppenberg HR, Chen G, Leisinger T & Cook AM (1995) Regulation of the degradative pathways from 4-toluenesulphonate and 4-toluenecarboxylate to protocatechuate in *Comamonas testosteroni* T-2. *Microbiology* **141**: 1891–1899.

Shimada T (2006) Xenobiotic-metabolizing enzymes involved in activation and detoxification of carcinogenic polycyclic aromatic hydrocarbons. *Drug Metab Pharmacokinet* **21**: 257–276.

Stamatakis A (2006) RAXML-VI-HPC: maximum likelihood-based phylogenetic analyses with thousands of taxa and mixed models. *Bioinformatics* **22**: 2688–2690.

Thurnheer T, Köhler T, Cook AM & Leisinger T (1986) Orthanilic acid and analogues as carbon sources for

bacteria: growth physiology and enzymic desulphonation. *J Gen Microbiol* **132**: 1215–1220.

Toledo FL, Calvo C, Rodelas B & Gonzalez-Lopez J (2006) Selection and identification of bacteria isolated from waste crude oil with polycyclic aromatic hydrocarbons removal capacities. *Syst Appl Microbiol* **29**: 244–252.

Tralau T, Cook AM & Ruff J (2001) Map of the IncP1β plasmid pTSA encoding the widespread genes (tsa) for *p*-toluenesulfonate degradation in *Comamonas testosteroni* T-2. *Appl Environ Microbiol* **67**: 1508–1516.

Tralau T, Yang EC, Tralau C, Cook AM & Kupper FC (2011) Why two are not enough: degradation of p-toluenesulfonate by a bacterial community from a pristine site in Moorea, French Polynesia. *FEMS Microbiol Lett* **316**: 123–129.

Turnbaugh PJ, Ley RE, Hamady M, Fraser-Liggett CM, Knight R & Gordon JI (2007) The human microbiome project. *Nature* **449**: 804–810.

Vitte I, Duran R, Hernandez-Raquet G, Mounier J, Jezequel R, Bellet V, Balaguer P, Caumette P & Cravo-Laureau C (2013) Dynamics of metabolically active bacterial communities involved in PAH and toxicity elimination from oil-contaminated sludge during anoxic/oxic oscillations. *Appl Microbiol Biotechnol* **97**: 4199–4211.

Zhao P, Yu KP & Lin CC (2011) Risk assessment of inhalation exposure to polycyclic aromatic hydrocarbons in Taiwanese workers at night markets. *Int Arch Occup Environ Health* **84**: 231–237.

Supporting Information

Additional Supporting Information may be found in the online version of this article:

Fig. S1. Sketch of B[*a*]P metabolism in eukaryotes (a) and prokaryotes (b), respectively.

Fig. S2. Transcription of DNA fragments found to be specific for B[*a*]P degradation *ex situ*.

Table S1. Primers for genes known or suspected to be involved in bacterial PAH degradation.